

Bmp6 and Bmp7 Are Required for Cushion Formation and Septation in the Developing Mouse Heart

Rebecca Y. Kim, Elizabeth J. Robertson,¹ and Mark J. Solloway²

Department of Molecular and Cellular Biology, Harvard University,
Cambridge, Massachusetts 02138

The mature heart valves and septa are derived from the cardiac cushions which initially form as local outgrowths of mesenchymal cells within the outflow tract and atrioventricular regions. Endocardial cells respond to signals from the overlying myocardium and undergo an epithelial-to-mesenchymal transformation to invade the intervening extracellular matrix. The molecules that can induce and maintain these cell populations are not known, but many candidates, including several TGF β s and BMPs, have been proposed based on their expression patterns and activities in other systems. In the present study, we describe the expression of *Bmp6* and *Bmp7* in overlapping and adjacent sites, including the cardiac cushions during mouse embryonic development. Previous analyses demonstrate that neither of these BMPs is required during cardiogenesis, but analysis of *Bmp6*;*Bmp7* double mutants uncovers a marked delay in the formation of the outflow tract endocardial cushions. A proportion of *Bmp6*;*Bmp7* mutants also display defects in valve morphogenesis and chamber septation, and the embryos die between 10.5 and 15.5 dpc due to cardiac insufficiency. These data provide the first genetic evidence that BMPs are involved in the formation of the cardiac cushions. © 2001 Academic Press

Key Words: BMP; TGF- β ; heart; endocardial cushion; mouse.

INTRODUCTION

The heart is the first functional organ in the vertebrate embryo. Paired mesodermal primordia migrate to the anterior–ventral midline where they fuse and undergo terminal differentiation (Rawles, 1943; Rosenquist and De Haan, 1966; Han *et al.*, 1992; Garcia-Martinez and Schoenwolf, 1993). Upon fusion, the primordia form a primitive linear heart tube consisting of an inner endothelium surrounded by a layer of myocardium (de la Cruz and Markwald, 1998). Between these tissues lies a complex layer of extracellular matrix known as the cardiac jelly produced mainly by the myocardium (Markwald *et al.*, 1975, 1977). Subsequent looping and morphogenesis of the linear heart tube leads to the formation of two sets of structurally distinct chambers, the atria and the ventricles. In addition, cells within the endocardium undergo a localized epithelial-to-mesenchymal transformation to become the endocardial cushions, precursors of

the valves and septa (Wessels *et al.*, 1996). Despite recent advances (Olson and Srivastava, 1996; Fishman and Chien, 1997), the molecular mechanisms that regulate these processes are not completely understood.

There is increasing evidence that secreted signaling molecules within the BMP subfamily of the TGF β superfamily are key regulators in the morphogenesis of multiple organ systems, including the heart (Kingsley, 1994; Hogan, 1996). *Decapentaplegic* (*Dpp*), a *Drosophila* homolog of *Bmp2* and *Bmp4*, is required for the expression of *tinman*, a mesoderm-specific homeobox gene (Bodmer *et al.*, 1990) necessary for midgut and heart formation (Azpiazu and Frasch, 1993; Bodmer, 1993). Consistent with this, the 3′-flanking region of the *tinman* gene contains binding sites for the Medea and Mad proteins (Xu *et al.*, 1998). These genes are members of the Smad family of molecules which have been shown to be essential mediators of TGF β -related signal transduction (Whitman, 1998). The expression of *tinman* in prospective cardiac mesoderm is significantly reduced in *Medea* mutant embryos, further implicating *Medea* in the activation of *tinman* in response to *Dpp* (Xu *et al.*, 1998). This pathway also appears to have been

¹ To whom correspondence should be addressed. Fax: (617) 496-6770. E-mail: ejrobert@fas.harvard.edu.

² Present address: Victor Chang Cardiac Research Institute, 384 Victoria Street, Darlinghurst NSW 2010 Australia.

conserved in the regulation of vertebrate cardiogenesis. Ectopic application of Bmp2 or Bmp4 to the noncardiogenic region of chick embryos induces early cardiac marker genes such as *GATA4*, *MHC*, and *Nkx2-5* (a vertebrate homolog of *tinman*), whereas inhibition of BMP signaling blocks later expression of *Nkx2-5* and cardiac differentiation (Schultheiss *et al.*, 1997; Andree *et al.*, 1998; Ladd *et al.*, 1998). Although cardiac induction does occur in mice deficient for Bmp2 (Zhang and Bradley, 1996) or the downstream effector molecule *Smad5* (Chang *et al.*, 1999; Yang *et al.*, 1999), subsequent growth and placement of the heart is aberrant in these embryos. These findings in *Drosophila* and vertebrates firmly establish the importance of BMP signaling in early cardiogenesis.

The TGF β superfamily has also been implicated in regulating the later stages of cardiac morphogenesis. Early in heart development, a subset of endothelial cells within the outflow tract (OT) and atrioventricular (AV) regions respond to signals emanating from the myocardium and differentiate into mesenchymal cells which migrate into the adjacent cardiac jelly (Mjaatvedt and Markwald, 1989). This endocardial cushion tissue later contributes to the mesenchymal components of the developing septa and valves of the heart. During murine endocardial cushion formation, TGF β 1 is expressed in endothelial/mesenchymal cells, while TGF β 2 and TGF β 3 are expressed in the myocardium (Akhurst *et al.*, 1990; Mahmood *et al.*, 1992; Dickson *et al.*, 1993, 1995). Specific interference with TGF β 3 signaling prevents the initial phenotypic changes normally seen in cushion formation in chicken embryos (Runyan *et al.*, 1992; Ramsdell and Markwald, 1997). Similar recent experiments demonstrate that the TGF β type III receptor, which lacks a recognizable signaling domain, acts as a permissive factor during this epithelial-mesenchymal transformation (Brown *et al.*, 1999). BMPs are also likely to be involved in the later processes of septation and valve formation (Eisenberg and Markwald, 1995; Yamagishi *et al.*, 1998). Bmp2, -4, -5, and -7 are strongly expressed in the developing myocardium of 8.5 dpc mouse embryos (Jones *et al.*, 1991; Lyons *et al.*, 1995b; Dudley and Robertson, 1997; Solloway and Robertson, 1999), whereas Bmp6 is expressed in both the OT myocardium and atrioventricular cushions (AVC) (Jones *et al.*, 1991; Dudley and Robertson, 1997). However, clear roles have yet to be established for these factors in cushion development. Targeted deletions of Bmp2 and Bmp4 cause lethality prior to cushion formation (Winnier *et al.*, 1995; Zhang and Bradley, 1996), and heart development is normal in embryos lacking Bmp5 (Kingsley *et al.*, 1992), Bmp6 (Solloway *et al.*, 1998), or Bmp7 (Dudley *et al.*, 1995; Luo *et al.*, 1995). However, a growing body of evidence indicates that BMPs potentially share redundant functions in several tissues.

Members of the TGF β superfamily are initially synthesized as precursor molecules whose intracellular dimerization, processing, and cleavage lead to the formation of mature signaling molecules (Massagué, 1998). Subunit composition can dramatically affect activity. For example,

in vitro-derived heterodimeric Bmp4/7 protein directly induces mesoderm in isolated *Xenopus* animal caps, whereas homodimeric proteins fail to induce any mesodermal markers (Nishimatsu and Thomsen, 1998). Additionally, BMP ligand/receptor binding appears to be promiscuous. Transfected cells expressing a single type I receptor, ALK-3, can bind Bmp2, Bmp4, Bmp6, and Bmp7 with varying affinities, depending on which Type II receptor is present (ten Dijke *et al.*, 1994; Ebisawa *et al.*, 1999). Genetic analyses further support these observations: embryos which are doubly mutant for distinct BMP family members often display unique phenotypes in tissues where the genes are normally coexpressed (Storm and Kingsley, 1996; Katagiri *et al.*, 1998; Solloway *et al.*, 1998; Solloway and Robertson, 1999). Taken as a whole, these results strongly argue that members of this gene family are likely to play redundant functions in tissues where they are coexpressed, such as the myocardium.

In the present study, we focus on a potent genetic interaction between mutations in two members of the 60A subfamily of BMPs, Bmp6 and Bmp7. These molecules share 87% amino acid identity in the mature C-terminal domain and are likely to signal via similar or identical downstream pathways. Both molecules can bind to cells expressing the Type-I receptors ALK-2, -3, or -6 (ten Dijke *et al.*, 1994; Ebisawa *et al.*, 1999) and can activate the downstream effectors Smad1 and Smad5 (Macias-Silva *et al.*, 1998; Ebisawa *et al.*, 1999). However, mutations in either gene cause very distinct phenotypes: Bmp6 mutants are homozygous viable and exhibit a slight delay in the growth of the sternum (Solloway *et al.*, 1998), while loss of Bmp7 function causes focal defects in the eye, kidney, and skeleton (Dudley *et al.*, 1995; Luo *et al.*, 1995). We identify several novel sites of Bmp6 expression during murine embryogenesis and compare the expression of Bmp6 and Bmp7 during heart formation. Analysis of Bmp6;Bmp7 double mutants uncovers a delay in formation of the OT cushions with subsequent valve and septation defects and a low penetrance exencephaly. These embryos die over a broad range of time due to cardiac insufficiency. Our results support a role for BMPs in regulating the growth of the cardiac cushions and myocardium.

MATERIALS AND METHODS

Mouse Strains

Mice carrying null alleles in Bmp6 (designated Bmp6^{miRob}) and Bmp7/lacZ and Bmp7 (designated Bmp7^{miRob}) have been previously described (Dudley *et al.*, 1995; Godin *et al.*, 1998; Solloway *et al.*, 1998) and were maintained independently on outbred backgrounds. To generate double-mutant mice, Bmp6 homozygous mice were crossed to Bmp7 heterozygotes to yield animals that were heterozygous for both Bmp6 and Bmp7. F₁ double heterozygotes were intercrossed to generate Bmp6^{-/-};Bmp7^{+/-} male stud mice, which were then crossed to doubly heterozygous or Bmp6^{-/-};Bmp7^{+/-} females in order to generate double-homozygous mutant embryos. The genotypes of live-born animals were determined by PCR

genotyping of DNA from tail tissue samples. For embryo collections, noon on the day of the appearance of the vaginal plug was considered 0.5 dpc. During the course of this study, no differences were noted among *Bmp6*^{+/-}; *Bmp7*^{+/-}, *Bmp6*^{-/-}, and wild-type embryos, so these groups were pooled for use as controls.

DNA Sample Collection and Genotyping Procedures

Yolk sac samples were collected during dissection, washed, and digested in 50 μ l yolk sac lysis buffer (50 mM KCl, 10 mM Tris—Cl, pH 8.3, 2.5 mM MgCl₂, 0.1 mg/ml gelatin, 0.45% NP-40, 0.45% Tween 20) containing 1.4 mg/ml Proteinase K overnight at room temperature. One microliter of digested material was PCR genotyped after boiling for 10 min. PCR genotyping of the targeted *Bmp6*, *Bmp7*, and *Bmp7/lacZ* alleles was carried out as described previously (Dudley *et al.*, 1995; Godin *et al.*, 1998; Solloway *et al.*, 1998).

Histology, β -Gal Staining, in Situ Hybridization, and TUNEL Analysis

Embryos were fixed in 4% paraformaldehyde in PBS at 4°C overnight, followed by dehydration through a graded methanol series. The embryos were cleared in xylene and embedded in paraffin wax. Samples were sectioned at 6–10 μ m and collected on Tespa-treated glass slides. Sections for histology were stained with hematoxylin and eosin using standard procedures. β -Gal staining was performed as described (Godin *et al.*, 1998). Conventional *in situ* hybridization of sections was performed as described (Jones *et al.*, 1991). Whole-mount *in situ* hybridization using digoxigenin-labeled RNA was performed (Wilkinson, 1992), and probes specific for *Bmp4* (Jones *et al.*, 1991), *Bmp6* (Lyons *et al.*, 1989b), *Bmp7* (Solloway *et al.*, 1998), *NF-ATc* (de la Pompa *et al.*, 1998), and *Desert Hedgehog* (Bitgood and McMahon, 1995) were used as described. Section TUNEL was carried out by using the Apoptag *in Situ* Apoptosis Detection Kit (Intergen, cat. no. S7101). For whole-mount antibody staining, embryos were collected and processed as indicated above. After rehydration into PBS, embryos were immunostained by using a 1:1000 dilution of rabbit anti-neurofilament 200 (Sigma Immunochemicals, cat. no. N4142) followed by a biotin-conjugated anti-rabbit secondary antibody. The Vectastain kit (Vector Laboratories) was used for final antigen detection by using DAB and hydrogen peroxide. All comparative photos were shot at identical resolutions.

BrdU Cell Proliferation Analysis

Pregnant females were injected with 0.1 mg of BrdU (Sigma, cat. no. B5002, at stock concentration of 10 mg/ml) per gram of body weight, and embryos were harvested 2 h postinjection. Embryos were fixed in Bouin's fixative overnight at 4°C, washed for several days in multiple changes of 70% ethanol, and then paraffin embedded. Eight-micrometer sections were mounted on Tespa-treated glass slides and immunostained with a 1:1000 dilution of anti-BrdU antiserum (Sigma, cat. no. P2531) followed by a biotin-conjugated anti-mouse secondary antibody. The Vectastain Elite kit (Vector Laboratories) was used for final antigen detection by using DAB and hydrogen peroxide. Sections were counterstained with hematoxylin. Mitotic index was calculated by counting relative numbers of BrdU-positive and -negative cells on scanned images from representative sections. Samples were counted twice,

and there was less than 2.5% variability per sample. A two-tailed F test was used to analyze the significance of variance between control and mutant samples. An unpaired Student's *t*-test was used to assess the significance of difference.

RESULTS

Colocalization of *Bmp6* and *Bmp7* Transcripts during Embryogenesis

The sites of *Bmp6* expression during mouse embryogenesis have been examined previously (Lyons *et al.*, 1989a,b; Jones *et al.*, 1991; Dudley and Robertson, 1997; Farrington *et al.*, 1997; Furuta *et al.*, 1997; Solloway *et al.*, 1998). However, during the course of this study, we observed several novel sites of *Bmp6* transcription. At 5.5 dpc, *Bmp6* transcripts are first observed in the extraembryonic endoderm (Fig. 1A). By 7.0 dpc, expression can be seen in the extraembryonic endoderm as well as rostral mesoderm (Figs. 1B and 1C). Later in embryogenesis (8.0 dpc, 8 somites), *Bmp6* mRNA is apparent in the foregut endoderm, caudal heart tube, and allantois (Fig. 1D). At 9.0 dpc (18 somites), in addition to these sites, *Bmp6* expression initiates in the branchial cleft ectoderm, ventral CNS, and forebrain neurectoderm at the telencephalic–diencephalic isthmus (Fig. 1E). This dorsal expression domain propagates caudally over two-thirds of the body axis by 10.0 dpc (Fig. 1F; Furuta *et al.*, 1997). Transcripts are also still apparent in the ectoderm at the base of the branchial arches, but this domain of expression disappears soon thereafter (data not shown). By the 40–45 somite stage, *Bmp6* is also detected in the mesenchyme at the rostral base of the forelimb bud (Fig. 1G) and in a similar position relative to the hindlimb bud at later stages (data not shown).

We also observed an interesting novel spatial restriction in *Bmp6* expression in the OT. As previously described, *Bmp6* mRNA is found in the myocardium of the OT at 9.5 dpc (Jones *et al.*, 1991; Dudley and Robertson, 1997). However, we noticed that transcript levels consistently appeared to decrease on the right side of the OT at 10.5 dpc (Fig. 1H) and were absent by 11.5 dpc (Fig. 1I). This was not due to a histological artifact as it was observed in multiple embryos, and a probe to *Bmp4* produced equal levels of signal on either side of the OT when hybridized to adjacent sections (data not shown). In addition, *Bmp6* expression at these stages reveals a difference in the development of anterior and posterior endocardial cushions: transcripts are readily detected in the mesenchyme of the AV cushions (Fig. 1J) but were never observed in the OT cushions at 11.5 dpc.

The expression patterns of *Bmp7* have also been extensively studied during murine development (Lyons *et al.*, 1995b; Arkell and Beddington, 1997; Dudley and Robertson, 1997; Furuta *et al.*, 1997; Shimamura and Rubenstein, 1997; Solloway *et al.*, 1998; Solloway and Robertson, 1999) and will be briefly reviewed here for comparison with *Bmp6*. *Bmp7* transcripts are first observed in the distal primitive streak at the onset of gastrulation (7.0 dpc), and this domain later expands to include the node and axial mesoderm.

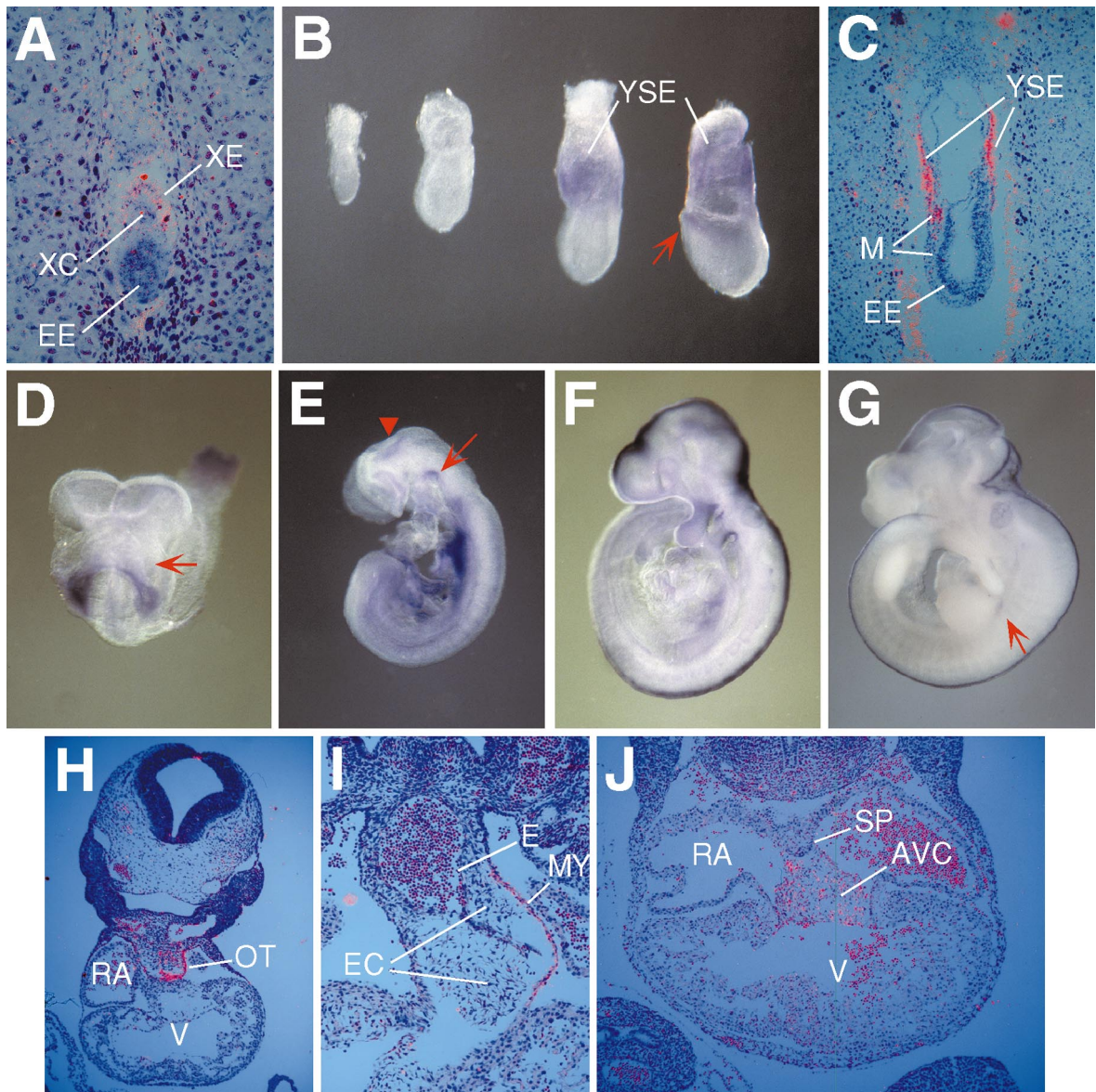


FIG. 1. Analysis of *Bmp6* expression in mouse embryos from 5.5 to 11.5 dpc by conventional (A, C, H–J) and whole-mount (B, D–G) *in situ* hybridization. Sagittal sections (A, C) and lateral view (B) of pregastrulation and gastrulation stage embryos. (A) *Bmp6* transcripts are first detected in extraembryonic endoderm at 5.5 dpc. (B, C) Expression is later observed in anterior cardiogenic mesoderm (arrow) and in the yolk sac endoderm at 7.0 dpc. (D) Eight-somite embryo showing expression of *Bmp6* in allantois, foregut endoderm, and ventral heart tube (arrow). (E) Expression persists in the gut and allantois at 9.0 dpc (18 somites). Expression also initiates in the dorsal diencephalon (arrowhead) and branchial cleft (arrow) at this stage. (F) By 10.0 dpc (25 somites), dorsal neural tube expression extends over two-thirds of the body axis. Transcripts are still detected in the ectoderm of the proximal branchial arch and cleft. (G) *Bmp6* is expressed in a small patch of mesenchyme at the base of the forelimb bud at 11.0 dpc (arrow). (H–J) Transverse sections through the heart at 10.5 dpc (H) and 11.5 dpc (I, J). Transcripts are detected in the myocardium of the proximal outflow tract (H, I) and atrioventricular cushion mesenchyme (J). AVC, atrioventricular cushion; E, cardiac endothelium; EC, endocardial cushion; EE, embryonic ectoderm; M, mesoderm; MY, myocardium; OT, outflow tract; RA, right atrium; SP, septum primum; V, ventricles; XC, extraembryonic ectoderm; XE, extraembryonic endoderm; YSE, yolk sac endoderm.

During gastrulation, *Bmp7* is expressed in extraembryonic endoderm of the visceral yolk sac and allantois as well as the embryonic cardiac and cranial mesoderm. By 8.5 dpc,

Bmp7 transcripts are apparent in the ectodermal components of the skin, optic vesicle, otic vesicle, and branchial arches in addition to the endoderm of the foregut and

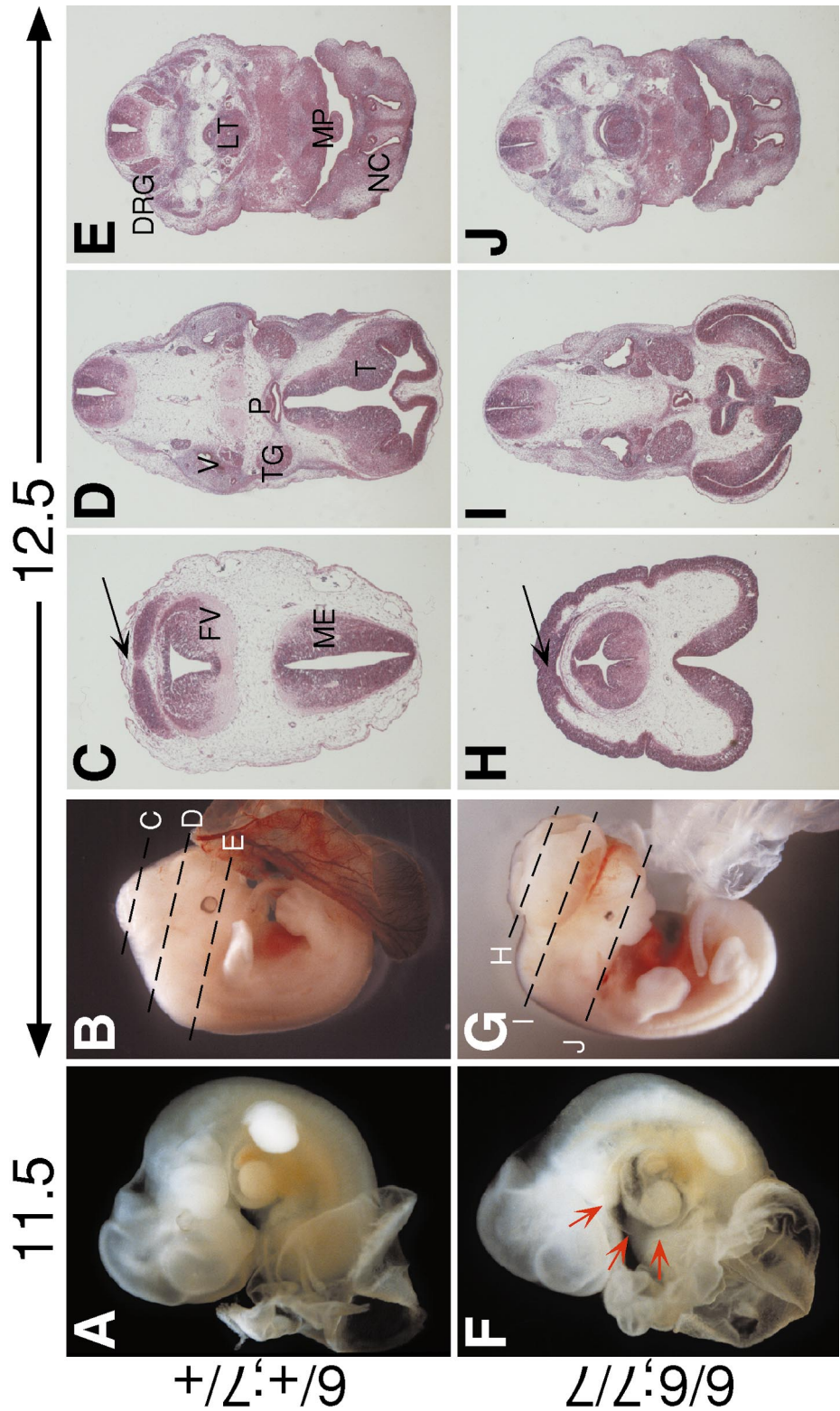


FIG. 2. Gross morphology of *Bmp6;Bmp7* mutants at 11.5 and 12.5 dpc. Comparison of control (A–E) and double-mutant (F–J) whole mounts (A, B, F, G) and sections (C–E, H–J). Transverse sections (C–E and H–J) correspond to regions in (B) and (G) marked by a dashed line. (A, F) *Bmp6;Bmp7* mutants display pericardial edema at 11.5 dpc (arrows). (B, G) A subset of 12.5 dpc mutants exhibit exencephaly (also see Table 1). Cranial histology in 12.5 dpc control (C–E) and mutant (H–J) embryos. Rostral diencephalon neuroectoderm fails to fuse dorsally and has wrapped over the metencephalon (arrow in H). This defect extends into the telencephalon (I), but *Bmp6;Bmp7* embryos are morphologically normal at the level of the nasal process (J). DRG, dorsal root ganglia; FV, fourth ventricle; LT, laryngo-tracheal groove; ME, mesencephalic vesicle of midbrain; MP, mandibular process; NC, nasal process; P, anterior lobe of pituitary; T, thalamus; TG, trigeminal ganglia; V, ventricle.

TABLE 1Onset of Gross Morphological Phenotype in *Bmp6*;*Bmp7* Double Mutant Embryos

Stage (dpc)	Total embryos	6/6;7/7 embryos	Open-head 6/6;7/7 embryos	Necrotic 6/6;7/7 embryos ^a	Developmentally delayed 6/6;7/7 embryos ^b
10.5	78	12	0	0	1 (8%)
11.5	97	21	0	3 (14%)	5 (24%)
12.5	207	29	7 (24%)	3 (10%)	1 (3%)
13.5–15.5	101	12	0	4 (33%)	0

Note. Embryos were collected and genotyped as described under Materials and Methods. Double mutants were recovered in Mendelian proportions at all stages.

^a Embryos with no heart peristalsis and pooled blood were classified as necrotic.

^b Developmentally delayed embryos were viable but their development lagged by at least 1 dpc.

hindgut pockets. *Bmp7* is also expressed in the neurectoderm of the telencephalon at this stage, and this expression domain later extends along the dorsal midline to a point caudal to the otic vesicle by 10.5 dpc. We confirmed this data by analyzing β -galactosidase activity in *Bmp7*/*lacZ* embryos and noted an interesting asymmetry within the myocardium of older embryos (data not shown). At 12.5 dpc, *Bmp7* expression appears to be down-regulated in the left atrium and ventricle ($n = 24$). No other asymmetries were noted in *Bmp7*/*lacZ* expression at these stages.

In sum, *Bmp6* and *Bmp7* are conspicuously coexpressed in several tissues during early embryogenesis, including the foregut and yolk sac endoderm, branchial arch ectoderm, dorsal neurectoderm of the brain, allantois mesenchyme, and OT myocardium. *Bmp6* and *Bmp7* are also expressed in adjacent cell populations in the roofplate and surface ectoderm, respectively. Since BMPs are secreted signaling factors, cells either within or cells adjacent to these tissues may potentially be affected by the combined loss of *Bmp6* and *Bmp7*.

***Bmp6*;*Bmp7* Mutants Develop Cardiac and Neural Defects**

In order to test whether *Bmp6* and *Bmp7* have shared functions during development, we generated mouse embryos which were doubly homozygous for mutant alleles of both genes. Outbred *Bmp7*^{miRob} heterozygotes (Dudley *et al.*, 1995) or *Bmp7*/*lacZ* heterozygotes (Godin *et al.*, 1998) were bred to *Bmp6*^{miRob} homozygotes (Solloway *et al.*, 1998). F₁ double heterozygotes were then backcrossed to *Bmp6* homozygotes to generate *Bmp6*^{-/-};*Bmp7*^{+/-} founders. All subsequent analysis was performed by using progeny from *Bmp6*^{-/-};*Bmp7*^{+/-} intercrosses, double heterozygote intercrosses, or crosses between *Bmp6*^{-/-};*Bmp7*^{+/-} founders and double heterozygotes. Of 134 newborn pups derived from crosses designed to yield *Bmp6*;*Bmp7* mice, none were double homozygous mutant for the *Bmp6* and *Bmp7* genes (approximately 34 were expected assuming Mendelian genetics). This result showed that the deletion of both genes caused prenatal lethality. In order to determine the time

point of embryonic failure and to ascertain the phenotypic defects in double-mutant embryos, dissections were initially carried out between 10.5 and 12.5 dpc, a period when significant overlap in the domains of *Bmp6* and *Bmp7* expression occur.

As shown in Table 1, the expected numbers of double homozygous mutants were recovered at 10.5 dpc assuming Mendelian inheritance. These embryos were overtly normal and indistinguishable from wild-type littermates, and histological analysis of eight double mutants failed to reveal any morphological defects. At 11.5 dpc, pericardial effusion and degeneration of cardiac tissue was apparent in 25% of the double mutants (Fig. 2F). By 12.5 dpc, 7 out of 29 double-mutant embryos were severely abnormal, frequently displaying an exencephalic midbrain and pericardial effusion (Fig. 2G). This phenotype was never seen in *Bmp6*^{-/-};*Bmp7*^{+/-} or *Bmp6*^{+/-};*Bmp7*^{-/-} littermates. Histological analysis demonstrates that the exencephaly is limited to the midbrain, whereas more caudal neural structures appear normal, including dorsal root ganglia and other neural crest-derived tissues (Figs. 2H–2J). Rostral sections reveal that the folds of the forebrain neurectoderm fail to fuse dorsally and subsequently become wrapped around the entire circumference of the head (Fig. 2H). The overall architecture of the brain is only mildly perturbed in the double mutant, appearing constricted from the lateral edges. The cephalic blood vessels are enlarged in the double mutants, but it is likely that this results secondarily from cardiac failure. *Bmp6* and *Bmp7* transcripts were never observed in the cranial blood vessels, although *Bmp6* expression was noted throughout the developing dorsal aorta and aortic/pulmonary trunks (Fig. 3, and data not shown). Posterior to the midbrain, the general tissue organization is similar between double mutant and controls (compare Fig. 2E with Fig. 2J).

BMP signaling has been implicated in the patterning of the dorsal neural tube (Liem *et al.*, 1995) as well as the generation and maintenance of neural crest cells (Graham *et al.*, 1994; Liem *et al.*, 1995; Arkell and Beddington, 1997). However, gross analysis of neuronal growth in double mutants via whole-mount antibody staining for neurofila-

ment failed to reveal any abnormalities aside from a reduction in neural projections near the eye (data not shown). This defect is likely due to the *Bmp7*-dependent microphthalmia (Dudley *et al.*, 1995). Immunocytochemistry experiments examining two subsets of dorsal commissural neurons, D1A and D1B, reveal no apparent defect in the differentiation of these interneurons in *Bmp6*, *Bmp7*, or *Bmp6;Bmp7* double mutants (K. Lee, T. Jessell, A. Dudley, M.J.S. and E.J.R., unpublished results), further confirming normal D/V patterning of the caudal CNS.

It was readily apparent that blood was not effectively circulating in the majority of double-mutant yolk sacs, despite the formation of robust blood vessels and obvious heart contractions. Statistical analysis of the numbers of the double mutants collected at 12.5 dpc fit Mendelian expectations, but the frequency of irretrievable embryonic resorptions and necrotic double mutants was increasing and the embryos that were retrieved were severely compromised. Thus, 12.5 dpc appears to be an important time point in the ontogeny of the *Bmp6;Bmp7* mutant phenotype. However, several double mutants were collected at later stages (13.5–15.5 dpc) which appeared morphologically normal and healthy aside from *Bmp7*-dependent microphthalmia and renal dysgenesis. Histological analysis of these embryos revealed normal development of tissues, including the brain, heart, and neural tube. In addition *Bmp7* expression was assessed by analyzing β -gal activity in six *Bmp6*^{-/-}; *Bmp7*^{lacZ/-} double mutants at 12.5 and 13.5 dpc. Previous analysis of β -gal activity in *Bmp7/lacZ* homozygous mutant embryos reveals that *Bmp7* expression is not autoregulative (Godin *et al.*, 1998), thus allowing its use as a marker in this study. Normal expression of the *lacZ* allele was observed in the surface ectoderm, AER, dorsal root ganglia, notochord, kidney tubules, metanephric mesenchyme, and myocardium (data not shown). Thus, we conclude that the majority of *Bmp6;Bmp7* mutant embryos die over a range of time (10.5–15.5 dpc) due to circulatory failure.

Bmp6 and Bmp7 mRNA Expression Patterns Abut and Overlap during Cardiac Development

The peripheral edema, restricted bloodflow, and broad range in timing of lethality suggested that *Bmp6* and *Bmp7* were required to maintain proper cardiac function. To better assess where and when coordinate signaling by these factors might be required during heart morphogenesis, we characterized their expression patterns in cardiac regions from 7.5 to 16.5 dpc (Fig. 3, and data not shown). *Bmp6* and *Bmp7* first become coexpressed after formation of the linear heart tube: *Bmp6* expression is localized to a small domain in the caudalmost aspect of the sinus venosus (Fig. 1D), while *Bmp7* is strongly expressed throughout the myocardium and sinus venosus (Dudley and Robertson, 1997; Solloway and Robertson, 1999) and continues to be expressed in the myocardium at all stages examined (Figs. 3B, 3D, 3F, and 3H). At 8.5 dpc, *Bmp6* is weakly expressed through all of the myocardium but is strongly expressed in

both the myocardium and endocardium of the OT (Fig. 3A). Expression persists in these two tissue layers at 9.5 dpc, but transcripts are no longer apparent in the myocardium of the ventricles and caudal bulbous cordis (Fig. 3C). As mentioned previously, *Bmp6* becomes expressed primarily within the left wall of the OT by 10.5 dpc (Fig. 1H). Later in development, *Bmp6* and *Bmp7* show an interesting pattern of adjacent expression domains during formation of the cardiac valves (Figs. 3E–3H). At 12.5 dpc, *Bmp6* transcripts highlight the valve leaflets, cushion mesenchyme of the aortico-pulmonary septum, and the endothelial lining of the pulmonary and aortic trunks (Fig. 3E), whereas *Bmp7* is expressed in the mesenchyme directly underlying the valve leaflets (Fig. 3F). These expression domains are also maintained at 14.5 dpc during the further elaboration of the valves (Figs. 3G and 3H). In summary, our data indicate that signaling by *Bmp6* and *Bmp7* may potentially interact early during myocardial development as well as later during valvuloseptal morphogenesis.

Double Mutants Exhibit a Delay in Formation of the Outflow Tract Cushions and Abnormal Valvo-Septation

Since acephalic embryos will survive to birth (Shawlot and Behringer, 1995), it seemed more likely that a defect in the heart or yolk sac could account for the lethality of the double mutants. During the process of dissection, it was observed that yolk sac morphology was variable between embryos: certain double mutants had robust blood vessels and blood flow in the yolk sac, while a significant proportion of embryos showed a lack of forward movement of blood through the vessels. Pericardial edema was clearly observed in several mutants at 11.5 dpc. Moreover, similar edema is also seen in embryos that die from cardiac defects as a result of other mutations (Chen *et al.*, 1994; Lyons *et al.*, 1995a) and was highly suggestive of a heart defect.

Examination of 11.5 dpc mutant heart sections reveals correct looping and septation of the heart tubes (Fig. 4). The atrio-ventricular cushions (AVC) and septum primum (SP), two tissues involved in the septation of the heart chamber into left and right atria and ventricles, form normally and are correctly placed within the heart. Intriguingly, the endocardial cushions of the OT were markedly underdeveloped in all double mutants (arrows in Fig. 4B; *n* = 12) compared to littermates (Fig. 4A; *n* = 6) and appeared to be in the early stages of epithelial-to-mesenchymal transformation, while the AVC were generally less compromised by the absence of *Bmp6* and *Bmp7* (Fig. 4H). Further examination of these and younger embryos revealed correct placement of the cushion outgrowths along the OT despite their reduced size. This observation was especially compelling considering that *Bmp6* and *Bmp7* are specifically coexpressed in the myocardium of the OT at this stage. In addition, double-mutant hearts often displayed reduced ventricular trabeculation (Figs. 4B and 4H). At 12.5 dpc, a comparison of serial sections through two healthy double

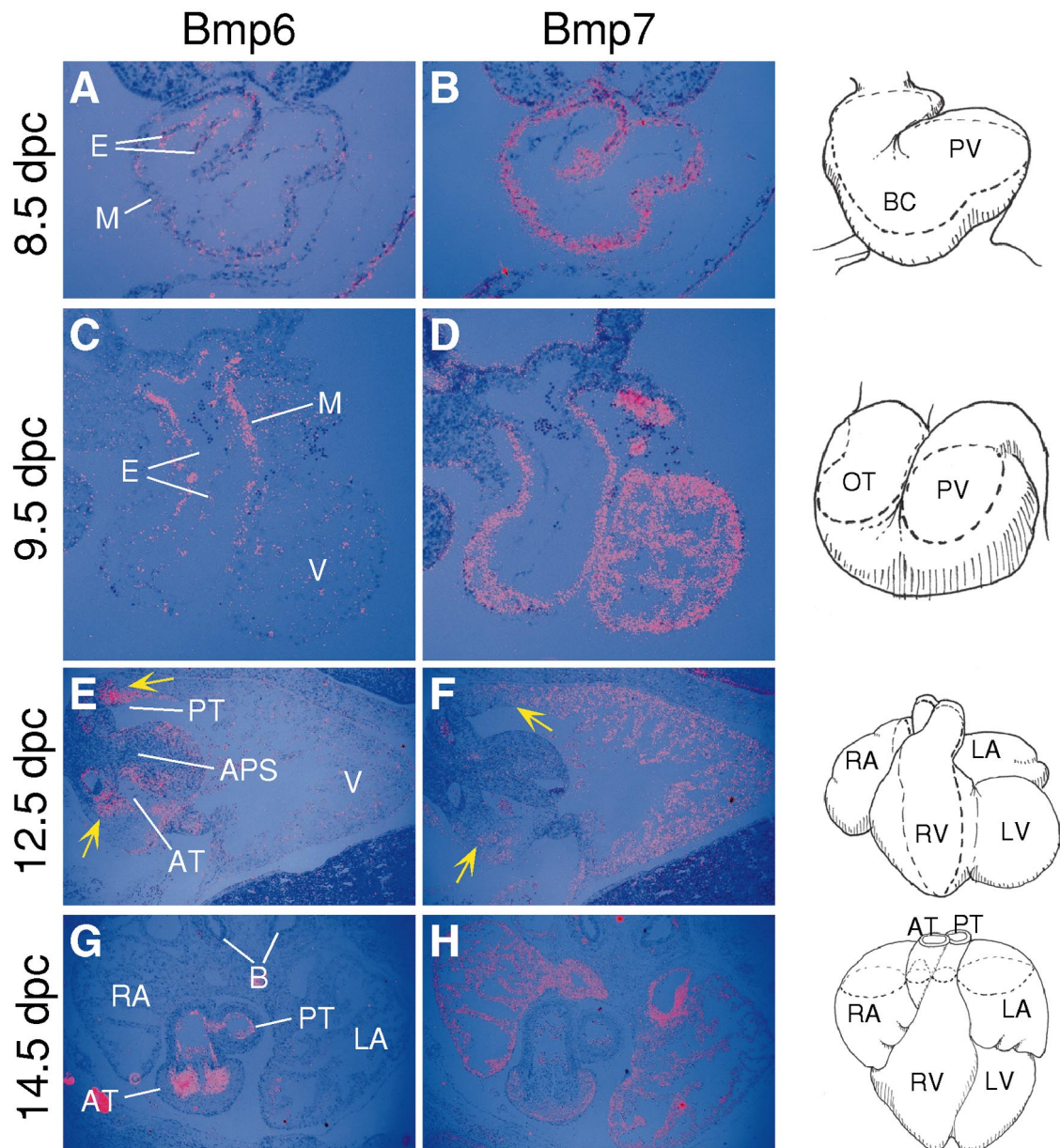


FIG. 3. Comparison of *Bmp6* and *Bmp7* expression in mouse embryos during cardiac development. The approximate location of the transverse (A–D, G, and H) and sagittal sections (E, F) is schematized on the right. (A) At 8.5 dpc, *Bmp6* is expressed in the myocardium and endocardium, whereas *Bmp7* transcripts are present throughout the myocardium at all stages examined (B, D, F, H). (C, D) At 9.5 dpc, *Bmp6* expression overlaps with *Bmp7* in the outflow tract myocardium. Transcripts are also still detected in the endothelium. (E) *Bmp6* is expressed in the endothelium and cushion mesenchyme (arrows) of the pulmonary and aortic trunks at 12.5 dpc, and (F) *Bmp7* transcripts are localized to regions of mesenchyme immediately adjacent to domains of *Bmp6* expression (arrows). (G, H) These expression domains persist at 14.5 dpc. *Bmp6* localizes to the aortic valve mesenchyme and endothelium of the pulmonary and aortic trunks, while *Bmp7* transcripts are found in the mesenchyme underlying the valves. A, atrium; AT, aortic trunk; APS, aortico-pulmonary spiral septum; B, bronchii; BC, bulbus cordis; E, cardiac endothelium; M, myocardium; OT, outflow tract; PT, pulmonary trunk; PV, primitive ventricle; V, ventricle.

mutants revealed normal development of the cushions (data not shown), suggesting either that these tissues were able to recover from the initial developmental retardation observed

at 11.5 dpc or that these embryos were only weakly affected by the mutations. However, the leaflets of the venous valve appeared to be displaced within the heart in these double

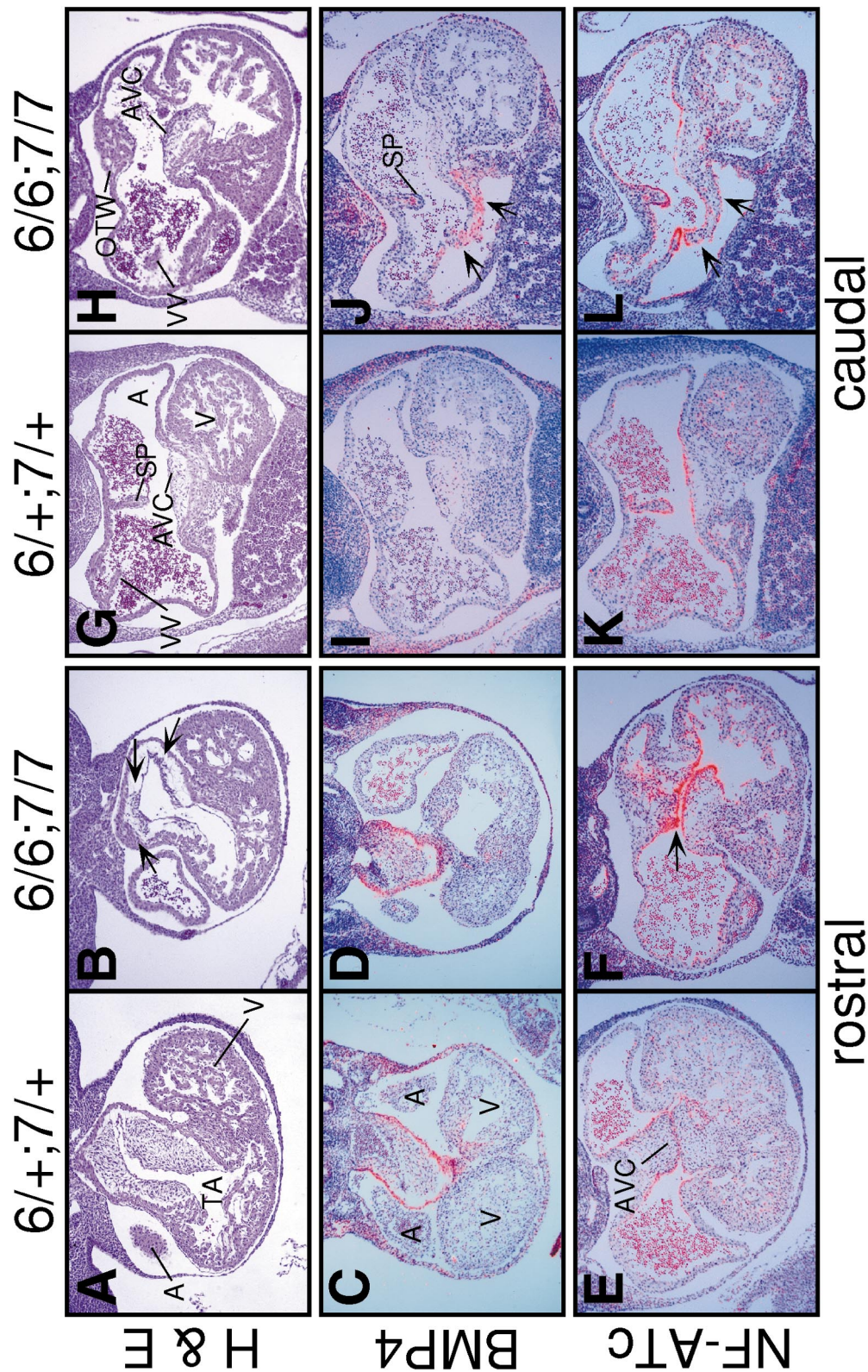


FIG. 4. Histology and marker analysis reveal abnormal morphogenesis of the endocardial cushions, valves, and septa in *Bmp6;Bmp7* double mutants at 11.5 dpc. Serial transverse sections taken from control (left) and *Bmp6;Bmp7* (right) littermates progress caudally from (A/B) to (K/L). Representative sections were hybridized with *Bmp4* (C, D, I, J) and *NF-ATc* (E, F, K, L). Apparent hybridization signal in atria is due to autofluorescence of blood. (A, B) Endocardial cushion outgrowth in the truncus arteriosus is severely delayed in *Bmp6;Bmp7* mutant embryos (arrows). (C, D) *Bmp4* is correctly localized to the myocardium of the truncus arteriosus in control and double mutants. (E, F) Endothelial *NF-ATc* expression outlines the atrioventricular cushions and further highlights their disorganization in *Bmp6;Bmp7* mutants (arrow). (G, H) Cushion tissue is displaced near the atrioventricular septum in the double mutant embryo (arrow). (I, J) *Bmp4* is incorrectly localized to cells adjacent to the atrioventricular cushions (arrows) and within the septum primum. No *Bmp4* expression is seen in the comparable wildtype sections. (K, L) *NF-ATc*-positive cells outline the displaced tissue near the venous valve (arrows) in the *Bmp6;Bmp7* mutant. A, atrium; AVC, atrioventricular cushion; OTW, outflow tract wall; SP, septum primum; TA, truncus arteriosus; V, ventricle; VV, leaflets of venous valve.

mutants. In addition, it was apparent in both double mutants that the atrial chamber and cardiac veins were abnormally dilated in comparison to littermates. This peripheral edema is likely to be secondary to congestive heart failure and valvular malfunction.

To gain a better understanding of the morphological defects observed in double-mutant hearts, we compared the expression patterns of *NF-ATc* (de la Pompa *et al.*, 1998), *Dhh* (Bitgood and McMahon, 1995), *Bmp4* (Jones *et al.*, 1991), and *Bmp6* (Lyons *et al.*, 1989b) at 10.5 and 11.5 dpc (Fig. 4; data not shown). Two wild-type and two double-mutant embryos were sectioned for *in situ* hybridizations at either stage, and the data collected were consistent between both groups. *NF-ATc* encodes a transcription factor required for proper valvo-septation, and is expressed throughout the endocardium from 7.5 to 11.5 dpc, whereas *Dhh* transcripts are restricted to the endocardium of the OT at 10.5 dpc. *Bmp4* and *Bmp6* colocalize to the myocardial layer of the OT, and *Bmp6* is also expressed in the AVC. In accordance with the results from our histological analyses, no significant differences were observed in the expression of these four genes at 10.5 dpc (data not shown). Furthermore, *Bmp4*, *Bmp6*, and *Dhh* were correctly localized in the OT of both *Bmp6;Bmp7* mutants at 11.5 dpc, indicating that the myocardium and endocardium of the OT were correctly specified. The proper restriction of *Bmp6* transcripts to cushion cells within the AV region (data not shown) indicates that the proximal/distal identity of cushion tissue is preserved despite delayed cushion growth in the OT. In contrast, although *Bmp4* was expressed normally in the OT myocardium (Figs. 4C and 4D), transcripts were aberrantly localized to cells surrounding the leaflets of the venous valve of the right atrium (Fig. 4J). Such expression has not been previously described for *Bmp4*, nor was it found in wild-type controls (Fig. 4I). The localization of *NF-ATc* transcripts within the endocardium lends further support to these observations. First, expression in the ventricle endocardium clearly reveals that trabeculation of the myocardium is less pronounced in *Bmp6;Bmp7* mutants at 11.5 dpc (Figs. 4E and 4F). Second, transcription in the endocardium surrounding the AVC highlights the disorganization of the cushions at the base of the double mutant truncus arteriosus (Fig. 4F). Finally, the abnormal *Bmp4*-expressing population of cells from Fig. 4J is also sheathed in *NF-ATc*-positive endothelium (Fig. 4L) and no analogous structure is present in control embryos (Fig. 4K). We conclude from these data that the processes of septation and valve placement are also affected by the absence of *Bmp6* and *Bmp7*.

In keeping with these observations, histological analysis of three viable 15.5 dpc *Bmp6;Bmp7* mutant embryos showed that each had a large ventricular septal defect (compare Figs. 5C with Figs. 5D and 5E). Growth of the muscular interventricular septum is believed to occur without contribution from the endocardial cushions, therefore it is likely that these defects reflect an additional requirement for *Bmp6* and *Bmp7* in the development of the early myocardium in addition to the OT. Interestingly, the dor-

sal, AVC-derived aspect of the septum was formed in all of the double mutants (Figs. 5D and 5E). Moreover, two of these embryos also displayed abnormal atrial septation (Fig. 5E), a process which does require cushion contribution. All three double mutants had formed pulmonary, tricuspid, mitral, and venous valves (Fig. 5, and data not shown), but the valves often appeared underdeveloped or misplaced. For example, in Fig. 5B, the pulmonary valve leaflets are much smaller in the double mutant than the control, whereas the tricuspid valve leaflets appear normal (Fig. 5F). Consistent with the condition of cardiac failure, the veins were dilated in two of the double mutants (Figs. 5B, 5D, and 5E). Another defect consistently noted in all three double-mutant embryos was the appearance of cystic spaces between the spinal cord and surrounding cartilaginous tissue immediately adjacent to the dorsal root ganglia (Fig. 5H). It is likely that these fluid-filled pockets arise secondarily from the cardiac defects, but they may also indicate localized regions of cellular degeneration. These spaces were only found occasionally in younger double mutants.

Cell Proliferation and Apoptosis in *Bmp6;Bmp7* Mutants

Potential explanations for the reduced size of the endocardial cushions in 11.5 dpc *Bmp6;Bmp7* mutant embryos include reduced proliferation of the cushion cells and/or a local increase in apoptosis. To distinguish between these two possibilities, we compared the levels of BrdU incorporation and TUNEL-positive cells in wild-type and mutant hearts at 11.5 dpc. No significant differences were found between the average percentage of proliferating cells in the endocardial cushions and neural tube (Figs. 6A–6G, and data not shown). Interestingly, unlike other tissues such as the neural tube or somites, cellular proliferation in the heart appears to only be coordinately regulated on a very gross level during this stage in development with dividing cells scattered throughout the atria and ventricles. Despite the reduced size of the cushions, OT mesenchymal cells continue to proliferate at this stage (Figs. 6C and 6D) and discrete cushion populations form appropriately along the length of the OT in double mutants (Figs. 6E and 6F). However, we did observe a large variance in the frequency of BrdU incorporation in the double-mutant OT cushions (24–45%) in comparison with the controls (31–35%) (Fig. 6G). F test analysis shows that double mutants display significant variability in BrdU labeling relative to controls ($F_{[7,5]} = 22.19$, $P = 0.0035$). These variances likely reflect abnormal growth regulation in these cells. As an internal control, BrdU incorporation was also assessed in the ventricular myocardium from the same sections, and we found that the mitotic index for the two double mutants was 22% ($n = 4167$ total cells) in comparison to 14% ($n = 4136$ total cells) for the two controls. The increased proliferation of the ventricular myocardium may be the cause of the muscular septal defects observed at 15.5 dpc. Despite this difference, in keeping with previous analyses, the mitotic index was

approximately 50% higher in the outer myocardial wall versus the trabeculae in both groups. Thus, the loss of *Bmp6* and *Bmp7* affects growth regulation in both the myocardium and endocardial cushions.

Serial sections were also collected from two littermates and two double mutants at 11.5 dpc to compare the levels of cell death by TUNEL. We found the localization of apoptotic cells to be identical between control and double mutant hearts at this stage, and thus we only present the wild-type data (Figs. 6H and 6I). In correlation with a recent study of apoptosis in the chicken embryo (Watanabe *et al.*, 1998), TUNEL-positive cells were localized to the OT myocardium immediately adjacent to the cushion mesenchyme at 11.5 dpc (Fig. 6H). Dying cells could also be seen in the interventricular septum (IVS). However, in contrast to the chick embryo, we failed to detect any TUNEL-positive cells in either mutant or wild-type endocardial cushions. In more caudal sections, apoptotic cardiomyocytes were found at the base of the AVC and within the IVS (Fig. 6I). We conclude that cellular proliferation within the heart is significantly perturbed in *Bmp6;Bmp7* mutants, whereas the patterns of apoptosis are largely unaffected.

DISCUSSION

Here, we have described the coexpression of *Bmp6* and *Bmp7* during murine embryogenesis from gastrulation onwards. *Bmp6;Bmp7* double mutants exhibit restricted defects in a subset of the tissues where expression of *Bmp6* and *Bmp7* overlaps. Significantly, these embryos display a pronounced delay in the morphogenesis of the OT endocardial cushions and die prenatally due to abnormal valvoseptation and cardiac insufficiency.

BMPs and Cushion Formation

The restricted delay in the growth of the endocardial cushions in *Bmp6;Bmp7* mutants is interesting considering the colocalization of these two growth factors within the OT myocardium prior to cushion formation. Signals from myocardial cells overlying the prospective cardiac cushions appear to induce the epithelial-to-mesenchymal transition of the invading endocardial cells leading to cardiac cushion formation (Wessels *et al.*, 1996). Recent experiments demonstrate that specific blockage of BMP-2 signaling using antisense oligodeoxynucleotides inhibits cushion mesenchyme formation in endocardium/myocardium cocultures (Yamagishi *et al.*, 1998) in a manner which parallels the defects in cushion growth seen in the *Bmp6;Bmp7* mutants. In addition to being coexpressed with *Bmp7* in the OT myocardial cells, *Bmp6* transcripts are also detected within the endocardial layer at 8.5 and 9.5 dpc. Thus, the localized expression of *Bmp6* may serve to regionally potentiate *Bmp7* signaling within the OT. It is tempting to speculate that these factors are directly involved in regulating epithelial-to-mesenchymal transformation during cushion

growth. However, many other BMPs are also expressed in the OT myocardium prior to cushion formation, including *Bmp2*, -4, -5, and -10 (Jones *et al.*, 1991; Lyons *et al.*, 1995b; Dudley and Robertson, 1997; Neuhaus *et al.*, 1999; Sollo-way and Robertson, 1999), and several type I receptors are ubiquitously expressed in the heart during cardiogenesis (Dewulf *et al.*, 1995; Ikeda *et al.*, 1996). Therefore, the endocardial cells of the OT are correctly positioned to receive signals provided by a potentially large number of BMP homo- and heterodimers.

The observation that disruption of BMP signaling fails to prevent cardiac induction but inhibits subsequent cardiomyocyte growth and induction (Shi *et al.*, 1997; Walters *et al.*, 2001) raises the possibility that the defects in cushion formation may also arise secondarily from myocardial dysfunction. *Bmp6;Bmp7* mutants display significantly variable proliferation rates in the OTC and increased proliferation of the myocardium at 11.5 dpc. The presence of atrial and ventricular septal defects in older double mutants provides further evidence of abnormal growth regulation throughout the myocardium. Discoordination of the relative rates of proliferation in the myocardium, endocardium, and cushion mesenchyme could provoke a delay in cushion formation by affecting signal crosstalk between these tissues, and this effect would be exacerbated if *Bmp6* and *Bmp7* were also involved in the further differentiation of the myocardium. Alternatively, these factors may affect cushion morphogenesis by regulating the proliferation of induced cushion cells. It is interesting to note that *Bmp6* expression is limited primarily to the developing OT region throughout cardiogenesis and is only weakly coexpressed with *Bmp7* in the entire myocardium at 8.5 dpc (Fig. 3). Thus, the combined absence of these two factors during early myocardium differentiation must eventually become manifest in abnormal cushion growth and chamber septation.

This paper and related studies indicate that, although superficially similar, several differences are apparent in the development of the AV and OT cushions. First, *Bmp6* is strongly expressed in mesenchymal cells of the AVC, whereas transcripts are not detected in the OTC at any stage examined (Fig. 1, and data not shown). Second, cushion mesenchyme along the OT was more affected by the combined loss of *Bmp6* and *Bmp7* than the mesenchyme of the AV region. This is likely due to the overlapping and adjacent expression of *Bmp6* and *Bmp7* within the OT endocardium and myocardium at 8.5 and 9.5 dpc. However, development of the AVC was slightly perturbed in the double mutants (Fig. 4). This abnormality may reflect segmental interactions between the adjacent AV and OT cushion populations or may be due to a limited requirement for both BMPs in the developing AVC. Next, as previously mentioned, several BMPs and TGF- β s are expressed only within the developing OT and not in the AV canal. Thus, endothelial/mesenchymal cells of the AVC and OTC are exposed to different milieus of secreted TGF- β factors. Expression of mammalian *Tolloid-like 1* (*mTLL-1*), a potential extracellular activator of BMPs, is seen within endocar-

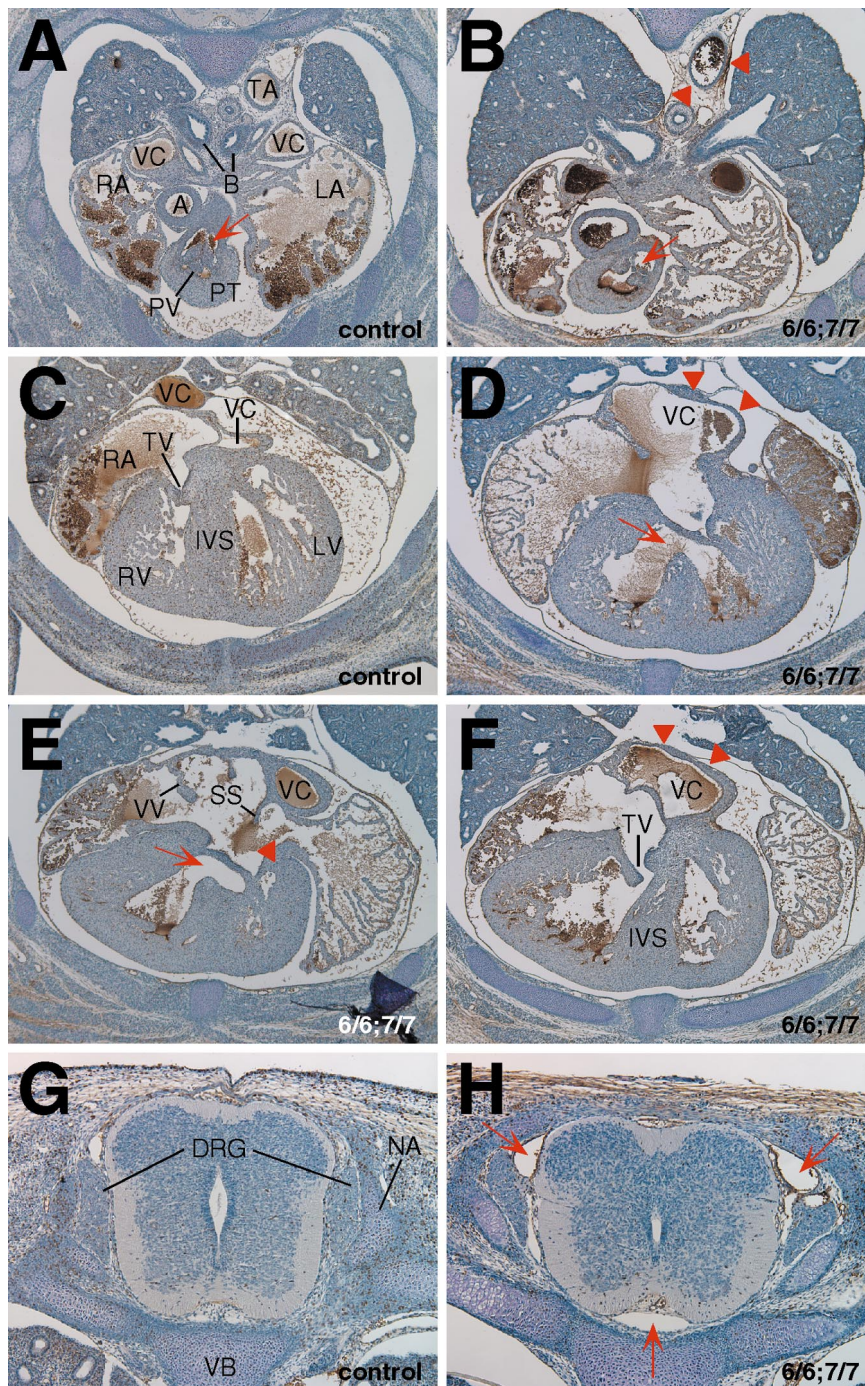


FIG. 5. Histological examination of cardiac abnormalities in *Bmp6;Bmp7* double mutants at 15.5 dpc by hematoxylin and peroxidase staining. Blood cells and extracellular matrix are stained brown by the peroxidase reaction. Transverse sections were collected from control (A, C, G) and double mutants (B, D–F, H). (B), (D), and (F) were taken serially from the same embryo. The aorta and pulmonary trunk are separate, with the pulmonary trunk connected to the thoracic aorta via the ductus arteriosus in both control (A) and *Bmp6;Bmp7* mutant embryos (B). However, the thoracic aorta is distended in the double mutant (arrowheads) and the pulmonary valve leaflets are misshapen (compare arrows in A and B). Sections collected more caudally reveal complete closure of the interventricular septum in controls (C), whereas the left and right ventricles remain connected in the double mutant (D) due to a failure in septation. The left superior vena cava is also distended in this embryo (arrowheads). (E) Sections through another double mutant show normal development of the vena cava and venous valve leaflets. However, this embryo contains balanced ventricular (arrow) and atrial (arrowhead) septal defects. The inferior component of the septum secundum is missing. (F) A caudal section from the same embryo in (B) and (D) shows partial closure of the interventricular septum, normal growth of the tricuspid valves (compare with B), and gross enlargement of the vena cava (arrowheads). (G, H) Transverse sections through the spinal cord overlying the heart region demonstrate formation of the dorsal root ganglia in control and mutant embryos. The double mutant displays pronounced cavities between the spinal cord and cartilaginous neural arch (arrows) which were never seen in control embryos. A, aorta; B, bronchus; DRG, dorsal root ganglion; IVS, interventricular septum; NA, neural arch; PT, pulmonary trunk; PV, pulmonary valve leaflet; R/LA, right/left atrium; R/LV, right/left ventricle; SS, septum secundum; TA, thoracic aorta; TV, tricuspid valve; VB, vertebral body; VC, superior vena cava; VV, venous valve of right superior vena cava.

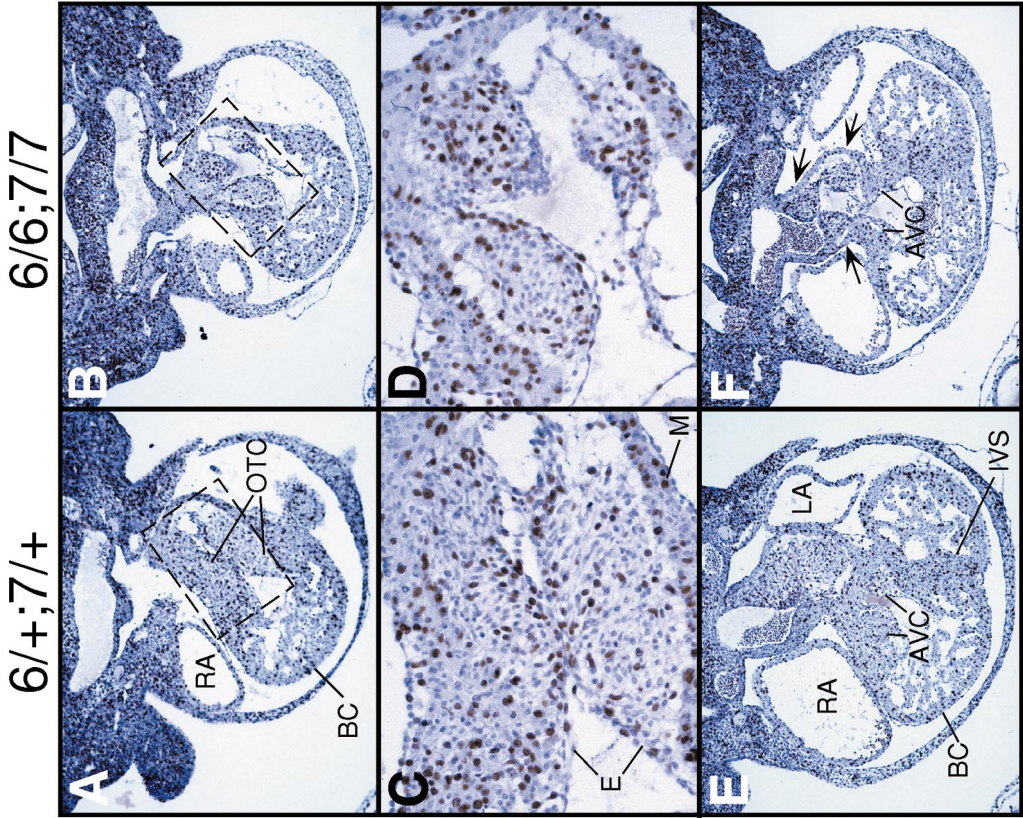


FIG. 6. Comparison of cellular proliferation and apoptosis within the heart at 11.5 dpc. BrdU incorporation was assessed in transverse sections through control (A, C, E) and double mutants (B, D, F). (A, B) Outgrowth of the endocardial cushion tissue is markedly delayed in double mutants. (C, D) High magnification views of the outflow tract cushions shown boxed in (A) and (B). Normal patterns of proliferation are apparent in the myocardium, cushion mesenchyme, and endothelium. (E, F) Proliferation is normal in caudal sections which include the atrioventricular cushions, interventricular septum, and trabeculae of the ventricles. In addition, localized cushion outgrowths are correctly localized within the OT. (G) Comparison of mitotic indices for OT cushion cells between two pairs of control and double mutant littermates. Data are presented as the ratio of BrdU-labeled cells \pm standard error of the mean. F test analysis shows that double mutants display significant variability in BrdU labeling relative to controls ($F_{(7,5)} = 22.19$, $P = 0.0035$). (H, I) TUNEL-labeling of rostral (H) and caudal (I) transverse sections through a control 11.5 dpc embryo. Identical results were obtained with Bmp6:Bmp7 mutant embryos (data not shown). (H) Small, localized patches of dying cells are apparent in the myocardium underlying the outflow tract cushions (arrows) and in the interventricular septum (arrowhead). (I) Apoptotic cells also lie beneath the atrioventricular cushions (arrow) and persist in the septum (arrowhead). AVC, atrioventricular cushion; BC, bulbus cordis; E, endothelium; IVS, interventricular septum; LA, left atrium; M, myocardium; RA, right atrium; OTC, outflow tract cushions.

dial cells lining the OT, but no expression is seen in the endocardial tissue of the atrioventricular canal (Clark *et al.*, 1999). Moreover, embryos lacking *mTLL-1* display multiple defects in heart positioning and septation (Clark *et al.*, 1999). Expression of *Smad6*, a putative negative regulator of BMP signaling, is restricted to the OT and AVC, and embryos lacking this gene develop excess cushion tissue, hyperplastic valves, and abnormal OT septation (Galvin *et al.*, 2000). This phenotype in effect complements the defects seen in the *Bmp6;Bmp7* double mutants; removal of a broad-spectrum BMP antagonist (*Smad6*) causes increased cushion cell production, whereas removal of two BMPs, one of which is localized to the OT, causes a reduction in the OT but not AV cushions. It is also likely that other BMPs present in these regions may obviate the severity of this phenotype. Although technically daunting, it would be very interesting to remove another OT-expressed BMP in the context of the *Bmp6;Bmp7* mutants to see the effect of reducing BMP signaling further. The recent discovery that *Smad6* is specifically induced by the BMP-responsive Smads, *Smad1* and *Smad5* (Ishida *et al.*, 2000), also prompts the speculation that *Smad6* is involved in an inhibitory feedback loop, controlling BMP activity during cushion morphogenesis. In sum, these data indicate that endothelial and cushion cells in the OT and AV regions are exposed to dramatically different combinations of BMP-related signals. It will be important to determine how these combined signals are interpreted during endocardial cushion formation.

Later Genetic Interactions between *Bmp6* and *Bmp7*

The mature inlet and outlet valve leaflets are composed of approximately equal amounts of mesenchymal and myocardial tissue, and the formation and integration of these two tissue types in the valve leaflets depends on the normal maturation of the cushion mesenchyme (Wunsch *et al.*, 1994; de la Cruz and Markwald, 1998). During the course of this study, we observed that severely affected *Bmp6;Bmp7* mutants display abnormalities in the positioning and formation of the venous valves which may be directly related to the cushion defects seen at 11.5 dpc. The delay in the production of *Bmp6;Bmp7* mutant OT cushion mesenchyme could impair the inductive interactions between this tissue and the myocardium. In addition, at a later stage (11.5 dpc), *Bmp6* is expressed within the proliferative zone of the valve mesenchyme, while *Bmp7* mRNA is detected in the more quiescent population of cells at the base of the valves (Fig. 3). Since TGF- β molecules have been shown to act over distances of several cell diameters (Ferguson and Anderson, 1992; Gurdon *et al.*, 1994), *Bmp6*- and *Bmp7*-dependent signals may potentially synergize at the interface between these two cell populations to regulate proliferation or directly influence transformation of the cushion into a valve. These questions remain to be investigated. Thus,

these defects could also reflect a requirement for BMPs during later stages of valve morphogenesis.

BMPs are expressed in the ectodermal cells adjacent to the neural plate (Liem *et al.*, 1995; Lyons *et al.*, 1995b; Arkell and Beddington, 1997; Dudley and Robertson, 1997; Furuta *et al.*, 1997; Solloway and Robertson, 1999) and roof plate differentiation appears to be mediated in part by BMPs (Liem *et al.*, 1995, 1997). Moreover, *Bmp4* has also been shown to induce *Msx* gene expression and apoptosis in presumptive neural crest cells from specific rhombomeres in the developing chick hindbrain (Graham *et al.*, 1994). The *Bmp6;Bmp7* exencephalic phenotype is interesting considering the overlapping expression of these factors in the dorsal midline of the forebrain and midbrain (Dudley and Robertson, 1997; Furuta *et al.*, 1997). However, the low penetrance of this defect (7/29 double mutants at 12.5 dpc) precluded further characterization. One attractive possibility is that this defect results from abnormalities in cell proliferation or apoptosis in the brain, but no differences were observed in BrdU incorporation or TUNEL in both exencephalic and "normal" double mutants (data not shown). Similarly, neuronal differentiation appeared unaffected by the loss of *Bmp6* and *Bmp7*.

Due to their coexpression along the dorsal midline overlying the branchial and pharyngeal arches, *Bmp6* and *Bmp7* may also potentially interact to influence neural crest formation. Cell-labeling experiments in cultured rodent models have been used to show that cardiac-specific neural crest cells originate within the posterior hindbrain, migrate to pharyngeal arches 3, 4, and 6, and from there populate the endocardial cushions of the OT (Fukiishi and Morriss-Kay, 1992; Serbedzija *et al.*, 1992). Elegant fate mapping studies reveal that this cell population subsequently contributes to part of the conotruncal septum and aortic valves (Jiang *et al.*, 2000). However, histological analysis of double mutant embryos from 10.5 to 12.5 dpc ($n = 12$) fails to reveal abnormalities in development of the arches or other neural crest-derived structures. Interestingly, despite clear evidence that division of the OT into the aorta and pulmonary trunk involves neural crest (Kirby and Waldo, 1995) and endocardial cushions (Webb *et al.*, 1998), persistent truncus arteriosus was never observed in double mutants at any stage, although this condition only arises after severe neural crest depletion. The delayed cushion morphogenesis observed in *Bmp6;Bmp7* mutants may implicate these factors in the recruitment of neural crest cells to the heart.

Mechanism of Interaction between Mutations in *Bmp6* and *Bmp7*

Several models can account for the genetic interactions observed between different BMP mutants. First, given the dimeric nature of TGF- β superfamily ligands, it has been proposed that the overlapping requirements for BMPs stem from the formation of heterodimeric molecules in cells that express both ligands (Israel *et al.*, 1996; Suzuki *et al.*, 1997; Nishimatsu and Thomsen, 1998). BMP heterodimers made

in vitro are significantly more active than homodimers in bone induction assays (Aono *et al.*, 1995; Israel *et al.*, 1996) and have opposing activities during mesoderm patterning in *Xenopus* (Suzuki *et al.*, 1997; Nishimatsu and Thomsen, 1998). The mechanism(s) by which heterodimers exert these effects have yet to be investigated; possible explanations include increased receptor affinity, resistance to degradation, and binding to novel receptor complexes. Aside from describing different levels of potency, none of the work to date has ascribed distinct activities to different heterodimer pairs, and the relevance of heterodimer signaling has yet to be determined *in vivo*. It is important to note too that the combined absence of Bmp6 and Bmp7 in cells would necessarily prevent the formation of both homodimers and Bmp6/Bmp7 heterodimers, as well as all other BMP heterodimers containing either Bmp6 or Bmp7. In contrast, deletion of only one BMP would only impinge on heterodimers containing that BMP. Deletion of two BMPs potentially removes a large, unique milieu of BMP heterodimers, and this cumulative loss of BMP signaling factors could then explain the synergism between these mutations.

Bmp6 and Bmp7 signaling may also potentially synergize at the level of cell-surface receptors or downstream effector molecules. Biochemical analyses of transfected and endogenous Type I receptors reveals that Bmp6 and Bmp7 share similar but distinct binding profiles. In general, both ligands bind strongly to Alk-2 and less tightly to Alk-3 and Alk-6; however, these results vary depending on the cells used (ten Dijke *et al.*, 1994; Macias-Silva *et al.*, 1998; Ebisawa *et al.*, 1999). In keeping with these observations, both Bmp6 and Bmp7 can activate endogenous Smad1 and Smad5, presumably via Alk-2 (Macias-Silva *et al.*, 1998; Ebisawa *et al.*, 1999). Intriguingly, blocking antiserum to Alk-2 inhibits endocardial transformation *in vitro* (Lai *et al.*, 2000). Thus, depending on the repertoire of Type I and Type II receptors, Smads and other effector molecules expressed in a given cell population, Bmp6 and Bmp7 homodimers have the capacity to elicit identical or similar downstream events.

Interaction between BMP and TGF- β Pathways

Several other members of the TGF- β superfamily, including Activin β A, TGF- β 1, β 2, and β 3, are differentially expressed within the heart during cushion formation and have been strongly implicated in regulating the endothelial-mesenchymal transformation (Akhurst *et al.*, 1990; Pelton *et al.*, 1991; Mahmood *et al.*, 1992; Dickson *et al.*, 1993; Moore *et al.*, 1998). In addition, Latent TGF- β -binding protein (LTBP-1), one component of a large extracellular latent TGF- β complex, is expressed throughout the extracellular matrix surrounding the cushions (Nakajima *et al.*, 1997). Specific interference with TGF- β 3 (Runyan *et al.*, 1992; Ramsdell and Markwald, 1997), TGF- β type III recep-

tor (TBR1) (Brown *et al.*, 1999), LTBP-1 (Nakajima *et al.*, 1997), or activin β A (Moore *et al.*, 1998) using either antisense oligonucleotides or blocking antibodies inhibits the initial stages of endocardial cushion growth. Intriguingly, misexpression of TBR1, which lacks a recognizable intracellular signaling domain, in nonresponsive ventricular endothelial cells conferred transformation in response to TGF- β 2 stimulation (Brown *et al.*, 1999). Moreover, TGF- β 2-null mice display defective valvoseptation (Sanford *et al.*, 1997) potentially caused by decreased proliferation of the OT myocardium or reduced contribution of neural crest cells. Collectively, this work provides compelling evidence that multiple TGF- β /activin signaling pathways play a role in cushion development. Our data, however, implicates a BMP-dependent signaling pathway in influencing similar processes in endocardial cushion transformation either directly or indirectly by affecting growth and/or differentiation of the myocardium. All evidence to date indicates that the downstream components of these two pathways are completely distinct from one another: Smads 1, 5, and 8 are R-Smads activated by BMP receptors, whereas Smad2 and Smad3 are activated by TGF- β and activin receptors (Massagué, 1998). How then can the OT endothelial and mesenchymal cells interpret and integrate these distinct signals to generate a similar outcome?

A potential answer to this problem was recently proposed by Yamagishi *et al.* (1998) who observed that while antisense oligonucleotides to Bmp2 inhibited endothelial-mesenchymal transformation in isolated OTs, addition of recombinant Bmp2 to cultured endothelial monolayers failed to trigger the initial stages of endothelial-mesenchymal transformation. Recombinant TGF- β 3, in contrast, elicits invasion and migration of endocardial cells *in vitro* (Ramsdell and Markwald, 1997), and Bmp2 treatment dramatically enhanced the response of cells to TGF- β 3. This synergism may explain why the delay in cushion growth observed in Bmp6;Bmp7 mutants closely mimics the effects of blocking TGF- β -dependent pathways. Precursor cells in the endocardium of the OT, which have already been "primed" by TGF- β signals, may proliferate more slowly in the absence of Bmp6 and Bmp7. If this hypothesis is correct, then it will be important to ascertain which ligands are specifically involved and how the TGF- β and BMP pathways converge within a responsive cell.

In the present study, we describe the coexpression of Bmp6 and Bmp7 at several sites during murine embryogenesis including the yolk sac, allantois, OT myocardium, foregut, and branchial arches. However, the primary defects in Bmp6;Bmp7 mutants are restricted to abnormalities in the morphogenesis of the OT cushions and incomplete chamber septation. Given the large number of TGF- β -related factors expressed in the developing OT myocardium and endocardium, these tissues can now be used to dissect the specific and/or overlapping activities of various ligands and downstream effector molecules.

ACKNOWLEDGMENTS

We thank Deepak Srivastava, Richard Harvey, and the anonymous reviewers for advice on heart development and useful discussions. We also thank Stuart Gilchrist for assistance with statistical analysis. We thank Thomas Yeoh, Rob Godin, Daniel Constam, and Leif Oxburgh for helpful comments on the manuscript, and Andy McMahon, Brigid Hogan, and Tak Mak for probes. We thank Patti Lewko and Joe Rocca for expert animal care and Debbie Pelusi for assistance with genotyping. M.J.S. was funded in part by an institutional NRSA training grant from the National Institutes of Health (T32-GM07620). This work was supported by a grant from the NIH (R01-HD25208) to E.J.R.

REFERENCES

- Akhurst, R. J., FitzPatrick, D. R., Gatherer, D., Lehnert, S. A., and Millan, F. A. (1990). Transforming growth factor β in mammalian embryogenesis. *Prog. Growth Factor Res.* **2**, 153–168.
- Andree, B., Duprez, D., Vorbusch, B., Arnold, H. H., and Brand, T. (1998). BMP-2 induces ectopic expression of cardiac lineage markers and interferes with somite formation in chicken embryos. *Mech. Dev.* **70**, 119–131.
- Aono, A., Hazama, M., Notoya, K., Taktomi, S., Yamasaki, H., Tsukuda, R., Sasaki, S., and Fujisawa, Y. (1995). Potent ectopic bone-inducing activity of Bone Morphogenetic Protein-4/7 heterodimer. *Biochem. Biophys. Res. Commun.* **210**, 670–677.
- Arkell, R., and Beddington, R. S. P. (1997). BMP-7 influences pattern and growth of the developing hindbrain of mouse embryos. *Development* **124**, 1–12.
- Azpiazu, N., and Frasch, M. (1993). tinman and bagpipe: Two homeobox genes that determine cell fates in the dorsal mesoderm of *Drosophila*. *Genes Dev.* **7**, 1325–1340.
- Bitgood, M. J., and McMahon, A. P. (1995). Hedgehog and Bmp genes are coexpressed at many diverse sites of cell–cell interaction in the mouse embryo. *Dev. Biol.* **172**, 126–138.
- Bodmer, R. (1993). The gene tinman is required for specification of the heart and visceral muscles in *Drosophila*. *Development* **118**, 719–729.
- Bodmer, R., Jan, L. Y., and Jan, Y. N. (1990). A new homeobox-containing gene, msh-2, is transiently expressed early during mesoderm formation of *Drosophila*. *Development* **110**, 661–669.
- Brown, C. B., Boyer, A. S., Runyan, R. B., and Barnett, J. V. (1999). Requirement of type III TGF- β receptor for endocardial cell transformation in the heart. *Science* **283**, 2080–2082.
- Chang, H., Huylebroeck, D., Verschueren, K., Guo, Q., Matzuk, M. M., and Zijnsen, A. (1999). Smad5 knockout mice die at mid-gestation due to multiple embryonic and extraembryonic defects. *Development* **126**, 1631–1642.
- Chen, Z., Friedrich, G. A., and Soriano, P. (1994). Transcriptional enhancer factor 1 disruption by a retroviral gene trap leads to heart defects and embryonic lethality in mice. *Genes Dev.* **8**, 2293–2301.
- Clark, T. G., Conway, S. J., Scott, I. C., Labosky, P. A., Winnier, G., Bundy, J., Hogan, B. L. M., and Greenspan, D. S. (1999). The mammalian Tolloid-like 1 gene, Tll1, is necessary for normal septation and positioning of the heart. *Development* **126**, 2631–2642.
- de la Cruz, M. V., and Markwald, R. R. (1998). “Living Morphogenesis of the Heart.” Springer-Verlag, Heidelberg.
- de la Pompa, J. L., Timmerman, L. A., Takimoto, H., Yoshida, H., Elia, A. J., Samper, E., Potter, J., Wakeham, A., Marengere, L., Langille, B. L., Crabtree, G. R., and Mak, T. W. (1998). Role of the NF-ATc transcription factor in morphogenesis of cardiac valves and septum. *Nature* **392**, 182–186.
- Dewulf, N., Verschueren, K., Lonnoy, O., Moren, A., Grimsby, S., Vande Spiegle, K., Miyazono, K., Huylebroeck, D., and ten Dijke, P. (1995). Distinct spatial and temporal patterns of two type I receptors for bone morphogenetic proteins during mouse embryogenesis. *Endocrinology* **136**, 2652–2653.
- Dickson, M. C., Martin, J. S., Cousins, F. M., Kulkarni, A. B., Karlsson, S., and Akhurst, R. J. (1995). Defective haematopoiesis and vasculogenesis in transforming growth factor- β 1 knockout mice. *Development* **121**, 1845–1854.
- Dickson, M. C., Slager, H. G., Duffie, E., Mummery, C. L., and Akhurst, R. J. (1993). RNA and protein localisations of TGF β 2 in the early mouse embryo suggest an involvement in cardiac development. *Development* **117**, 625–639.
- Dudley, A. T., Lyons, K. M., and Robertson, E. J. (1995). A requirement for bone morphogenetic protein-7 during development of the mouse mammalian kidney and eye. *Genes Dev.* **9**, 2795–2807.
- Dudley, A. T., and Robertson, E. J. (1997). Overlapping expression domains of bone morphogenetic protein family members potentially account for limited tissue defects in *BMP7* deficient embryos. *Dev. Dyn.* **208**, 349–362.
- Ebisawa, T., Tada, K., Kitajima, I., Tojo, K., Sampath, T. K., Kawabata, M., Miyazono, K., and Imamura, T. (1999). Characterization of bone morphogenetic protein-6 signaling pathways in osteoblast differentiation. *J. Cell Sci.* **112**, 3519–3527.
- Eisenberg, L. M., and Markwald, R. R. (1995). Molecular regulation of atrioventricular valvuloseptal morphogenesis. *Circ. Res.* **77**, 1–6.
- Farrington, S. M., Belaousoff, M., and Baron, M. H. (1997). Winged-helix, Hedgehog and BMP genes are differentially expressed in distinct cell layers of the murine yolk sac. *Mech. Dev.* **62**, 197–211.
- Ferguson, E. L., and Anderson, K. V. (1992). Decapentaplegic acts as a morphogen to organize dorsal-ventral pattern in the *Drosophila* embryo. *Cell* **71**, 451–461.
- Fishman, M. C., and Chien, K. R. (1997). Fashioning the vertebrate heart: Earliest embryonic decisions. *Development* **124**, 2099–2117.
- Fukiishi, Y., and Morriss-Kay, G. M. (1992). Migration of cranial neural crest cells to the pharyngeal arches and heart in rat embryos. *Cell Tissue Res.* **268**, 1–8.
- Furuta, Y., Piston, D. W., and Hogan, B. L. M. (1997). Bone morphogenetic proteins (BMPs) as regulators of dorsal forebrain development. *Development* **124**, 2203–2212.
- Galvin, K. M., Donovan, M. J., Lynch, C. A., Meyer, R. I., Paul, R. J., Lorenz, J. N., Fairchild-Huntress, V., Dixon, K. L., Dunmore, J. H., Gimbrone, M. A., Jr., Falb, D., and Huszar, D. (2000). A role for smad6 in development and homeostasis of the cardiovascular system. *Nat. Genet.* **24**, 171–174.
- Garcia-Martinez, V., and Schoenwolf, G. C. (1993). Primitive-streak origin of the cardiovascular system in avian embryos. *Dev. Biol.* **159**, 706–719.
- Godin, R. E., Takaesu, N. T., Robertson, E. J., and Dudley, A. T. (1998). Regulation of BMP7 expression during kidney development. *Development* **125**, 3473–3482.

- Graham, A., Francis-West, P., Brickell, P., and Lumsden, A. (1994). The signaling molecule BMP-4 mediates apoptosis in the rhombencephalic neural crest. *Nature* **372**, 684–686.
- Gurdon, J. B., Harger, P., Mitchell, A., and Lemaire, P. (1994). Activin signalling and response to a morphogen gradient. *Nature* **371**, 487–492.
- Han, Y., Dennis, J. E., Cohen-Gould, L., Bader, D. M., and Fischman, D. A. (1992). Expression of sarcomeric myosin in the presumptive myocardium of chicken embryos occurs within six hours of myocyte commitment. *Dev. Dyn.* **193**, 257–265.
- Hogan, B. L. M. (1996). Bone morphogenetic proteins: Multifunctional regulators of vertebrate development. *Genes Dev.* **10**, 1580–1594.
- Ikeda, T., Takahashi, H., Suzuki, A., Ueno, N., Yokose, S., Yamaguchi, A., and Yoshiki, S. (1996). Cloning of rat type I receptor cDNA for bone morphogenetic protein-2 and bone morphogenetic protein-4, and the localization compared with that of the ligands. *Dev. Dyn.* **206**, 318–329.
- Ishida, W., Hamamoto, T., Kusanagi, K., Yagi, K., Kawabata, M., Takehara, K., Sampath, T. K., Kato, M., and Miyazono, K. (2000). Smad6 is a Smad1/5-induced smad inhibitor. Characterization of bone morphogenetic protein-responsive element in the mouse Smad6 promoter. *J. Biol. Chem.* **275**, 6075–6079.
- Israel, D. I., Nove, J., Kerns, K. M., Kaufman, R. J., Rosen, V., Cox, K. A., and Wozney, J. M. (1996). Heterodimeric bone morphogenetic proteins show enhanced activity in vitro and in vivo. *Growth Factors* **13**, 291–300.
- Jiang, X., Rowitch, D. H., Soriano, P., McMahon, A. P., and Sucov, H. M. (2000). Fate of the mammalian cardiac neural crest. *Development* **127**, 1607–1616.
- Jones, C. M., Lyons, K. M., and Hogan, B. L. M. (1991). Involvement of Bone Morphogenetic Protein-4 (BMP-4) and *Vgr-1* in morphogenesis and neurogenesis in the mouse. *Development* **111**, 531–542.
- Katagiri, T., Boorla, S., Frendo, J. L., Hogan, B. L. M., and Karsenty, G. (1998). Skeletal abnormalities in doubly heterozygous *Bmp4* and *Bmp7* mice. *Dev. Genet.* **22**, 340–348.
- Kingsley, D. M. (1994). The TGF- β superfamily: New members, new receptors, and new genetic tests of function in different organisms. *Genes Dev.* **8**, 133–146.
- Kingsley, D. M., Bland, A. E., Grubber, J. M., Marker, P. C., Russell, L. B., Copeland, N. G., and Jenkins, N. A. (1992). The mouse short ear skeletal morphogenesis locus is associated with defects in a bone morphogenetic member of the TGF β superfamily. *Cell* **71**, 399–410.
- Kirby, M. L., and Waldo, K. L. (1995). Neural crest and cardiovascular patterning. *Circ. Res.* **77**, 211–215.
- Ladd, A. N., Yatskievych, T. A., and Antin, P. B. (1998). Regulation of avian cardiac myogenesis by activin/TGF β and bone morphogenetic proteins. *Dev. Biol.* **204**, 407–419.
- Lai, Y. T., Beason, K. B., Brames, G. P., Desgrosellier, J. S., Cleggett, M. C., Shaw, M. V., Brown, C. B., and Barnett, J. V. (2000). Activin receptor-like kinase 2 can mediate atrioventricular cushion transformation. *Dev. Biol.* **222**, 1–11.
- Liem, K. F., Tremml, G., Roelink, H., and Jessell, T. M. (1995). Dorsal differentiation of neural plate cells induced by BMP-mediated signals from epidermal ectoderm. *Cell* **82**, 969–979.
- Liem, K. F. J., Tremml, G., and Jessell, T. M. (1997). A role for the roof plate and its resident TGF β -related proteins in neuronal patterning in the dorsal spinal cord. *Cell* **91**, 127–138.
- Luo, G., Hofmann, C., Bronckers, A. L. J. J., Sohocki, M., Bradley, A., and Karsenty, G. (1995). BMP-7 is an inducer of nephrogenesis, and is also required for eye development and skeletal patterning. *Genes Dev.* **9**, 2808–2820.
- Lyons, I., Parsons, L. M., Hartley, L., Li, R., Andrews, J. E., Robb, L., and Harvey, R. P. (1995a). Myogenic and morphogenetic defects in the heart tubes of murine embryos lacking the homeobox gene *Nkx2-5*. *Genes Dev.* **9**, 1654–1666.
- Lyons, K., Graycar, J. L., Lee, A., Hashmi, S., Lindquist, P. B., Chen, E. Y., Hogan, B. L. M., and Derynck, R. (1989a). *Vgr-1*, a mammalian gene related to *Xenopus Vg-1*, is a member of the transforming growth factor β gene superfamily. *Proc. Natl. Acad. Sci. USA* **86**, 4554–4558.
- Lyons, K. M., Hogan, B. L. M., and Robertson, E. J. (1995b). Colocalization of BMP 7 and BMP 2 RNAs suggests that these factors cooperatively mediate tissue interactions during murine development. *Mech. Dev.* **50**, 71–83.
- Lyons, K. M., Pelton, R. W., and Hogan, B. L. M. (1989b). Patterns of expression of murine *Vgr-1* and BMP-2a RNA suggest that transforming growth factor- β -like genes coordinately regulate aspects of embryonic development. *Genes Dev.* **3**, 1657–1668.
- Macias-Silva, M., Hoodless, P. A., Tang, S. J., Buchwald, M., and Wrana, J. L. (1998). Specific activation of Smad1 signaling pathways by the BMP7 type I receptor, ALK2. *J. Biol. Chem.* **273**, 25628–25636.
- Mahmood, R., Flanders, K. C., and Morriss-Kay, G. M. (1992). Interactions between retinoids and TGF β s in mouse morphogenesis. *Development* **115**, 67–74.
- Markwald, R. R., Fitzharris, T. P., and Manasek, F. J. (1977). Structural development of endocardial cushions. *Am. J. Anat.* **148**, 85–119.
- Markwald, R. R., Fitzharris, T. P., and Smith, W. N. (1975). Structural analysis of endocardial cytodifferentiation. *Dev. Biol.* **42**, 160–180.
- Massagué, J. (1998). TGF- β signal transduction. *Annu. Rev. Biochem.* **67**, 753–791.
- Mjaatvedt, C. H., and Markwald, R. R. (1989). Induction of an epithelial-mesenchymal transition by an in vivo adheron-like complex. *Dev. Biol.* **136**, 118–128.
- Moore, C. S., Mjaatvedt, C. H., and Gearhart, J. D. (1998). Expression and function of activin β A during mouse cardiac cushion tissue formation. *Dev. Dyn.* **212**, 548–562.
- Nakajima, Y., Miyazono, K., Kato, M., Takase, M., Yamagishi, T., and Nakamura, H. (1997). Extracellular fibrillar structure of latent TGF β binding protein-1: Role in TGF β -dependent endothelial-mesenchymal transformation during endocardial cushion tissue formation in mouse embryonic heart. *J. Cell Biol.* **136**, 193–204.
- Neuhaus, H., Rosen, V., and Thies, R. S. (1999). Heart specific expression of mouse BMP-10 a novel member of the TGF- β superfamily. *Mech. Dev.* **80**, 181–184.
- Nishimatsu, S., and Thomsen, G. H. (1998). Ventral mesoderm induction and patterning by bone morphogenetic protein heterodimers in *Xenopus* embryos. *Mech. Dev.* **74**, 75–88.
- Olson, E. N., and Srivastava, D. (1996). Molecular pathways controlling heart development. *Science* **272**, 671–676.
- Pelton, R. W., Saxena, B., Jones, M., Moses, H. L., and Gold, L. I. (1991). Immunohistochemical localization of TGF β 1, TGF β 2, and TGF β 3 in the mouse embryo: Expression patterns suggest multiple roles during embryonic development. *J. Cell Biol.* **115**, 1091–1105.
- Ramsdell, A. F., and Markwald, R. R. (1997). Induction of endocardial cushion tissue in the avian heart is regulated, in part, by TGF β -3-mediated autocrine signaling. *Dev. Biol.* **188**, 64–74.

- Rawles, M. E. (1943). The heart-forming areas of the early chick blastoderm. *Physiol. Zool.* **41**, 22–42.
- Rosenquist, G. C., and De Haan, R. L. (1966). Migration of precardiac cells in the chick embryo: A radioautographic study. *Carnegie Inst. Washington Contrib. Embryol.* **38**, 111–121.
- Runyan, R. B., Potts, J. D., and Weeks, D. L. (1992). TGF- β 3-mediated tissue interaction during embryonic heart development. *Mol. Reprod. Dev.* **32**, 152–159.
- Sanford, L. P., Ormsby, I., Gittenberger-de Groot, A. C., Sariola, H., Friedman, R., Boivin, G. P., Cardell, E. L., and Doetschman, T. (1997). TGF β 2 knockout mice have multiple developmental defects that are non-overlapping with other TGF β knockout phenotypes. *Development* **124**, 2659–2670.
- Schultheiss, T. M., Burch, J. B., and Lassar, A. B. (1997). A role for bone morphogenetic proteins in the induction of cardiac myogenesis. *Genes Dev.* **11**, 451–462.
- Serbedzija, G. N., Bronner-Fraser, M., and Fraser, S. E. (1992). Vital dye analysis of cranial neural crest cell migration in the mouse embryo. *Development* **116**, 297–307.
- Shawlot, W., and Behringer, R. R. (1995). Requirement for Lim1 in head-organizer function. *Nature* **374**, 425–430.
- Shi, Y., Hata, A., Lo, R. S., Massagué, J., and Pavletich, N. P. (1997). A structural basis for mutational inactivation of the tumour suppressor Smad4. *Nature* **388**, 87–93.
- Shimamura, K., and Rubenstein, J. L. (1997). Inductive interactions direct early regionalization of the mouse forebrain. *Development* **124**, 2709–2718.
- Solloway, M. J., Dudley, A. T., Bikoff, E. K., Lyons, K. M., Hogan, B. L. M., and Robertson, E. J. (1998). Mice lacking Bmp6 function. *Dev. Genet.* **22**, 321–39.
- Solloway, M. J., and Robertson, E. J. (1999). Early embryonic lethality in Bmp5;Bmp7 double mutant mice suggests functional redundancy within the 60A subgroup. *Development* **126**, 1753–1768.
- Storm, E. E., and Kingsley, D. M. (1996). Joint patterning defects caused by single and double mutations in members of the bone morphogenetic protein (BMP) family. *Development* **122**, 3969–3979.
- Suzuki, A., Kaneko, E., Maeda, J., and Ueno, N. (1997). Mesoderm induction by BMP-4 and -7 heterodimers. *Biochem. Biophys. Res. Commun.* **232**, 153–156.
- ten Dijke, P., Yamashita, H., Sampath, T. K., Reddi, A. H., Estevez, M., Riddle, D. L., Ichijo, H., Heldin, C. H., and Miyazono, K. (1994). Identification of type I receptors for osteogenic protein-1 and bone morphogenetic protein-4. *J. Biol. Chem.* **269**, 16985–16988.
- Walters, M. J., Wayman, G. A., and Christian, J. L. (2001). Bone morphogenetic protein function is required for terminal differentiation of the heart but not for early expression of cardiac marker genes. *Mech. Dev.* **100**, 263–273.
- Watanabe, M., Choudhry, A., Berlan, M., Singal, A., Siwik, E., Mohr, S., and Fisher, S. A. (1998). Developmental remodeling and shortening of the cardiac outflow tract involves myocyte programmed cell death. *Development* **125**, 3809–3820.
- Webb, S., Brown, N. A., and Anderson, R. H. (1998). Formation of the atrioventricular septal structures in the normal mouse. *Circ. Res.* **82**, 645–656.
- Wessels, A., Markman, M. W., Vermeulen, J. L., Anderson, R. H., Moorman, A. F., and Lamers, W. H. (1996). The development of the atrioventricular junction in the human heart. *Circ. Res.* **78**, 110–117.
- Whitman, M. (1998). Smads and early developmental signaling by the TGF β superfamily. *Genes Dev.* **12**, 2445–2462.
- Wilkinson, D. G. (1992). "Whole-Mount in Situ Hybridization of Vertebrate Embryos." IRL Press, Oxford.
- Winnier, G., Blessing, M., Labosky, P. A., and Hogan, B. L. M. (1995). Bone morphogenetic protein-4 is required for mesoderm formation and patterning in the mouse. *Genes Dev.* **9**, 2105–2116.
- Wunsch, A. M., Little, C. D., and Markwald, R. R. (1994). Cardiac endothelial heterogeneity defines valvular development as demonstrated by the diverse expression of JB3, an antigen of the endocardial cushion tissue. *Dev. Biol.* **165**, 585–601.
- Xu, X., Yin, Z., Hudson, J. B., Ferguson, E. L., and Frasch, M. (1998). Smad proteins act in combination with synergistic and antagonistic regulators to target Dpp responses to the Drosophila mesoderm. *Genes Dev.* **12**, 2354–2370.
- Yamagishi, T., Nakajima, Y., Sampath, T. K., Miyazono, K., and Nakamura, H. (1998). Bone morphogenetic protein 2 acts synergistically with transforming growth factor β 3 in endothelial-mesenchymal cell transformation during chick heart development. *Ann. N. Y. Acad. Sci.* **857**, 276–278.
- Yang, X., Castilla, L. H., Xu, X., Li, C., Gotay, J., Weinstein, M., Liu, P. P., and Deng, C. X. (1999). Angiogenesis defects and mesenchymal apoptosis in mice lacking SMAD5. *Development* **126**, 1571–1580.
- Zhang, H., and Bradley, A. (1996). Mice deficient for BMP2 are nonviable and have defects in amnion/chorion and cardiac development. *Development* **122**, 2977–2986.

Submitted for publication November 1, 2000

Revised March 30, 2001

Accepted March 30, 2001

Published online June 13, 2001